Acta Materialia 175 (2019) 477–486

Contents lists available at ScienceDirect

Acta Materialia

journal homepage: www.elsevier.com/locate/actamat

Full length article

Asymmetric cyclic response of tensile pre-deformed Cu with highly oriented nanoscale twins

Qingsong Pan [a, 1], Haofei Zhou [b, c, 1], Qiuhong Lu [a], Huajian Gao [c, **], Lei Lu [a, *]

[a] Shenyang National Laboratory for Materials Science, Institute of Metal Research, Chinese Academy of Sciences, Shenyang, 110016, PR China
[b] Department of Engineering Mechanics, Zhejiang University, Hangzhou, 310027, PR China
[c] School of Engineering, Brown University, Providence, RI, 02912, USA

ARTICLE INFO

Article history:
Received 22 January 2019
Received in revised form
28 May 2019
Accepted 15 June 2019
Available online 18 June 2019

Keywords:
Nanotwin
Pre-strain effect
Asymmetric cyclic response
Correlated necklace dislocations
Fatigue mechanism

ABSTRACT

History-independent, stable and symmetric cyclic response has been detected in as-deposited bulk polycrystalline Cu with highly oriented nanotwins [Nature 551 (2017) 214–217]. In this study, to deepen the understanding of cyclic deformation in nanotwinned (NT) structures, small levels of tensile pre-strains were applied on NT-Cu, followed by strain-controlled symmetric tension-compression cyclic tests. Distinct from the symmetric cyclic response of as-deposited NT-Cu, the magnitude of the maximum stress in tension is much larger than that of the minimum stress in compression, indicating that the cyclic response of tensile pre-deformed NT-Cu is highly asymmetric. The degree of its cyclic asymmetry gradually decays as the number of cycles or the plastic strain amplitude is increased. The tensile pre-deformed NT-Cu recovers to its symmetric cyclic response after cyclic deformation at sufficiently large plastic strain amplitude, analogous to that detected in as-deposited NT counterparts. Molecular dynamics simulations and microstructural observations revealed that the observed asymmetric cyclic response is mainly related to the activation and movement of threading dislocations with extended misfit dislocation tails lying on the twin boundaries (TBs) during tensile pre-deformation. During cyclic deformation, threading dislocations in adjacent twin interiors tend to link their long tails with one another to form correlated necklace dislocations (CNDs) with a symmetric structure. The CNDs move back-and-forth along the twin boundaries without directional slip resistance, contributing to the transition from asymmetric to symmetric cyclic response of NT-Cu.

1. Introduction

Most service failures of metallic components are caused by progressive defects and fatigue damage accumulation in the materials under cyclic stresses/strain [1]. Traditional coarse-grained (CG) metals always exhibit inferior fatigue properties such as very low fatigue limit, mainly owing to their low strength [1,2]. Over the past two decades, various ultra-fine grained (UFG) and nanocrystalline metals have been investigated and found to exhibit an enhanced strength and fatigue limit [3–7]. However, these materials typically exhibit cyclic softening and shorter strain-controlled fatigue life due to severe strain localization via local grain coarsening and shear banding [4,8,9], which severely limit their engineering applications because of safety concerns [10].

Recently, it has been shown that introducing a high density of highly oriented nanotwins embedded within micrometer-sized grains can be regarded as an effective strategy to achieve desirable tensile strength [11–17], substantial ductility and work hardening in metallic materials [18,19]. Under cyclic loading, NT metals exhibit an extremely high fatigue limit under stress control [20,21], an enhanced fatigue life under strain control and a suppressed fatigue crack growth rate, in distinct contrast to the trade-off trend between high cycle and low cycle fatigue performance of twin-free CG and UFG counterparts [22,23].

Most interestingly, a history-independent and stable cyclic response was reported in bulk Cu samples with highly oriented nanoscale twins [24], distinct from conventional unstable cyclic response and strain localizing cyclic mechanisms associated with cumulative, irreversible microstructural damage in single-crystal [25–27], CG [1,25,28,29], UFG and nanograined metals [4,5,10].

* Corresponding author.
** Corresponding author.
E-mail addresses: huajian_gao@brown.edu (H. Gao), llu@imr.ac.cn (L. Lu).
[1] These authors contributed equally to this work.

https://doi.org/10.1016/j.actamat.2019.06.026
1359-6454/

The uniqueness of the history-independent cyclic stress-strain behavior of NT-Cu lies in that the cyclic stress response behavior is not only independent of the plastic strain amplitude with a wide range (from 0.02% to 0.25%) but also independent of strain magnitude sequence and cyclic number under a series of step-by-step strain amplitudes [24]. This is quite different from the history-independent cyclic stress-strain curve obtained in the conventional annealed and pre-strained wavy slip materials like Cu, as pioneered by Feltner and Laird [30] and frequently discussed in the literature [31,32]. In these cases, overlapping cyclic stress-strain curves in the saturation stage are achieved mainly for individual constant strain amplitude. In the original work of Feltner and Laird, only rather large plastic strain amplitudes in the range of 0.5%–5% were employed. Later, Lukáš and Klesnil showed that, in the range of much smaller plastic strain amplitudes below 0.1%, the cyclic stress-strain behavior of copper is no longer independent of the mechanical prehistory [33]. Thus, in the present context, it is remarkable that NT-Cu, in contrast to conventional copper, has earlier been shown to exhibit a history-independent cyclic stress-strain response at rather small plastic strain amplitudes down to 0.02% [24]. Taking all facts together, the history-independent cyclic stress-strain behavior of NT-Cu is considered to be truly unique.

We demonstrated that this unusual history-independent fatigue behavior of NT-Cu is governed by a type of mobile, single-slip and super-stable correlated necklace dislocations (CNDs) formed by linking threading dislocations in neighboring nanotwin interiors under cyclic loading. The NT structure is cyclically stable as long as the nanotwins are tilted within about 15° relative to the loading axis [24].

In real service conditions, materials in engineering components may undergo a very complex pre-loading history, such as stamping of automotive body, which will strongly influence subsequent cyclic behaviors [1,30,33–35]. Therefore, the pre-deformation history seems to be of great importance for materials during subsequent cyclic loading.

In this study, as a first step, we confine to a rather simple tensile pre-deformation with small strains as our experimental strategy. It has been demonstrated that the movement of threading dislocations inside the individual twin channels dominates plastic deformation of NT Cu in uniaxial tensile tests with the loading axis approximately parallel to the twin planes [36,37]. So, we impose small amount of tensile strains on the NT-Cu specimens to introduce threading dislocations, and then investigate the effect of pre-existing threading dislocations on the subsequent cyclic behavior by fully reversed tension-compression with constant strain amplitudes. The cyclic responses, especially the symmetric/asymmetric behavior of tensile pre-deformed NT-Cu were systematically investigated by experiments and simulations.

2. Methods

2.1. Experimental details

Bulk high purity copper (99.99 wt%) sheets containing highly oriented nanoscale growth twins are synthesized by means of direct-current electro-deposition technique in an electrolyte of $CuSO_4$. The substrate is a pure Ti sheet. The final thickness of NT-Cu plates is ~3.4 mm. For comparison, twin-free UFG-Cu samples are produced by cold rolling high purity (99.99 wt%) CG-Cu samples with a rolling strain of $\varepsilon = (t_0 - t)/t = 450\%$, where t_0 and t denote the thickness of the initial and the as-rolled samples, respectively. To produce CG-Cu samples with grain size similar to that of NT-Cu samples, the as-obtained UFG-Cu samples are annealed at 250 °C for 2 h in air. More details about sample preparation are described in Ref. [23].

Dog-bone shaped specimens are cut from NT-, UFG- and CG-Cu sheets with a gauge cross-section area of 4×3 mm^2 and a length of 12 mm by using electrical spark machine. All specimens are mechanically ground to the desired dimensions, followed by electro-polishing to obtain smooth surfaces with negligible surface roughness.

Uniaxial tensile pre-deformation and symmetrical tension-compression tests of NT-, CG- and UFG-Cu samples are performed on an Instron 8874 testing machine at room temperature in air. For NT-Cu samples, the loading axis is approximately parallel to most of the twin planes. A dynamic strain gauge extensometer (Instron Catalogue No. 2620–603) with a gauge length of 10 mm is clamped on the specimen surface for accurate direct measurement and closed-loop control of strain during tensile and cyclic tests. The strain resolution and control precision are smaller than 0.01%. The samples were initially deformed to tensile pre-strains of 1.5% and 3%, respectively. After unloading, symmetric tension-compression tests were performed under three different plastic strain amplitudes ($\Delta\varepsilon_{pl}/2$) ranging from 0.02%, 0.05%–0.15%, respectively. The number of cycles is 70 for each $\Delta\varepsilon_{pl}/2$. For comparison, the tension-compression cyclic responses of the samples are also measured without pre-deformation treatments.

The cross-sectional microstructures of the Cu specimens before and after tensile and fatigue tests were characterized by a FEI Tecnai F20 transmission electron microscope (TEM) operated at 200 kV. A two-beam diffraction technique in TEM was used to characterize the dislocations in twin interiors [38]. The TEM foils were prepared by the following scheme: the sample was first sliced parallel to the loading axis by electrical spark machining, and mechanically polished to a thickness of ~40 μm. It was finally thinned by twin-jet polishing in an electrolyte of phosphoric acid (25%), alcohol (25%) and deionized water (50%) at about −10 °C.

2.2. Molecular dynamics simulations

The simulated NT-Cu sample is $[1\bar{1}1]$ textured and composed of 4 columnar grains with a mean grain size of 50 nm. The grains have in-plane orientations of 1°, 27°, 47° and 89° with respect to the x-axis, and out-of-plane translations of 5 nm, 10 nm, 15 nm and 20 nm with respect to the x-y plane. Each grain has four subgrain nanotwins with non-uniform thicknesses of 2 nm, 3 nm, 6 nm and 12 nm. The sample contains a total of 20 million atoms and have dimensions of $100 \times 100 \times 23$ nm^3. For comparison, a twin-free polycrystalline sample with the same columnar grain morphology is also investigated.

The sample is first equilibrated at 300 K for 300 ps. Uniaxial tensile or compressive loading is applied along the y-axis using a displacement-controlled method, while zero pressure is ensured along the non-stretching directions. The maximum applied strain is 15% for both tension and compression pre-loadings. The sample is unloaded to zero stress and equilibrated for 200 ps before cyclic loading. Three different total strain amplitudes of $\Delta\varepsilon_t/2 = 0.5\%$, 1% and 2% are used for symmetric tension-compression cyclic loading, respectively. The maximum and minimum stresses, σ_{max} and σ_{min}, are recorded in each cycle.

Throughout the simulations, periodic boundary conditions are used for all dimensions. All simulations were performed at a temperature of 300 K controlled by Nose-Hoover thermostat and barostat [39,40], which allows thermal activation of dislocations in the simulated NT samples. The embedded atom method potential is used to describe the interatomic interactions [41]. The time step is 1 fs. The strain rate is 1×10^9 s^{-1}.

Common-neighbor analysis method [42] is used to identify lattice defects in the samples, which are visualized based on two different methods. One method is based on the crystal structure:

green for fcc atoms with perfect crystal structure, red for hcp atoms in twin boundaries and stacking faults, grey for disordered atoms in dislocation cores and grain boundaries [43,44]. The second method is a position-based coloring scheme in which colors are assigned to atoms based on their spatial coordinates [24,45].

We have used MD simulations to complement our experimental studies in revealing the cyclic deformation mechanisms of pre-deformed NT metals. However, it should be mentioned that there still exists a large discrepancy in both spatial and temporal scales between MD simulations and experiments. The high strain rates and small dimensions applied in MD simulations are known to cause substantial quantitative differences and may even lead to qualitative difference in the simulated results as compared to the experimental results. A typical MD simulation can only consider metallic samples containing up to hundreds of millions of atoms that are deformed within a few nanoseconds. The strain rates in MD simulations are about 10 orders of magnitude higher than those in experiments, implying limited relaxation time for atomic motion and defect activation. Thus, MD simulations can result in significantly higher macroscopic stresses than in experiment [46]. Hence, caution must be exerted when comparing MD simulation results with experiment. In particular, deformation mechanisms identified by MD simulations must be carefully verified through systematic TEM observations. This was done in the present work.

3. Results

3.1. Cyclic symmetry of NT-, CG- and UFG-Cu without tensile pre-deformation

Most polycrystalline grains in as-deposited bulk NT-Cu samples are columnar in shape and subdivided by nanoscale twin lamellae parallel to the deposition plane [21,36]. The mean grain size of NT-Cu used in this study is ~6.1 μm and its mean twin thickness is ~64 nm. The ultrafine grains in cold-rolled UFG-Cu samples are elongated with a mean transverse grain size of ~0.38 μm. The mean grain size of annealed CG-Cu samples is ~9.8 μm, which is comparable to that of NT-Cu samples.

NT-, UFG- and CG-Cu samples without pre-deformation treatments are cyclically deformed at three individual constant plastic strain amplitudes $\Delta\varepsilon_{pl}/2 = 0.02\%$, 0.05% and 0.15%. Taking $\Delta\varepsilon_{pl}/2 = 0.05\%$ for instance, the stress-strain hysteresis loops of as-deposited NT-Cu (without pre-deformation) at different cycles nearly overlap with each other (Fig. 1a). This is typical of stable cyclic response of NT-Cu samples observed under various $\Delta\varepsilon_{pl}/2$ [23]. In contrast, we observed cyclic softening in UFG-Cu (Fig. 1b) and cyclic hardening in CG-Cu (Fig. 1c).

Besides, Fig. 1a shows that the magnitude of the maximum stress in tension (σ_{max}) of NT-Cu samples is almost identical to that of the minimum stress in compression (σ_{min}), indicating a symmetric cyclic response under symmetric tension-compression loading of NT-Cu samples. Cyclic symmetry was also observed in CG-Cu and UFG-Cu. The gap between σ_{max} and $|\sigma_{min}|$ is only ~2 MPa in CG Cu (Fig. 1b) and it increases to ~50 MPa in UFG Cu (Fig. 1c), but both are much smaller than the magnitude of their σ_{max} and σ_{min} (i.e., ~71 MPa and ~326 MPa at 70th cycle). The above results suggest that without pre-deformation treatments, cyclic symmetry under symmetric tension-compression loading is common to Cu samples with various microstructures. Similar symmetric cyclic response is also universally reported in other conventional fcc monocrystal [26,47,48] and CG [1,30,49–52] metals with different grain sizes, cyclically deformed at different constant strain amplitudes.

3.2. Cyclic response of NT-, UFG- and CG-Cu after tensile pre-deformation

In order to investigate the effect of tensile pre-deformation on the cyclic behavior of NT structure, NT-Cu is first subjected to a tensile pre-strain of 1.5% at which the tensile stress reaches 467 MPa (Fig. 2a). The tensile pre-deformation is followed by three individual fully reversed tension-compression cyclic loading tests with $\Delta\varepsilon_{pl}/2$ equal to 0.02% (Fig. 2b and e), 0.05% (Fig. 2c and f) and 0.15% (Fig. 2d and g). Fig. 2b shows that, for $\Delta\varepsilon_{pl}/2 = 0.02\%$, the stress-strain hysteresis loops of NT-Cu at different cycles overlap, but are highly asymmetric with respect to the origin of the coordinates. For every single cycle, the maximum stress σ_{max} is ~216 MPa, while the minimum stress σ_{min} is only −42 MPa, forming a stress gap as large as ~174 MPa (Fig. 2e). The observed cyclic tension-compression asymmetry in NT-Cu induced by tensile pre-deformation is fundamentally distinct from the symmetric responses of as-deposited NT-Cu during cyclic deformation (Fig. 1a) and conventional fcc CG metals reported in the literature [1,48,53].

Asymmetric cyclic response is also detected in tensile pre-deformed NT-Cu at larger $\Delta\varepsilon_{pl}/2$ (Fig. 2c,d, f and g). For example, the maximum and the minimum stresses of NT-Cu cyclically deformed at $\Delta\varepsilon_{pl}/2 = 0.05\%$ are 243 MPa and −80 MPa at the first cycle, respectively, leading to a stress gap of (σ_{max} - $|\sigma_{min}|$) = 163 MPa (Fig. 2f). It is observed that the stress gap decreases gradually with increasing number of cycles at $\Delta\varepsilon_{pl}/2 = 0.05\%$ and 0.15%, indicating a reduced degree of cyclic asymmetry due to cyclic deformation (Fig. 2f and g). Moreover, increasing the imposed $\Delta\varepsilon_{pl}/2$ from 0.05% to 0.15% reduces the

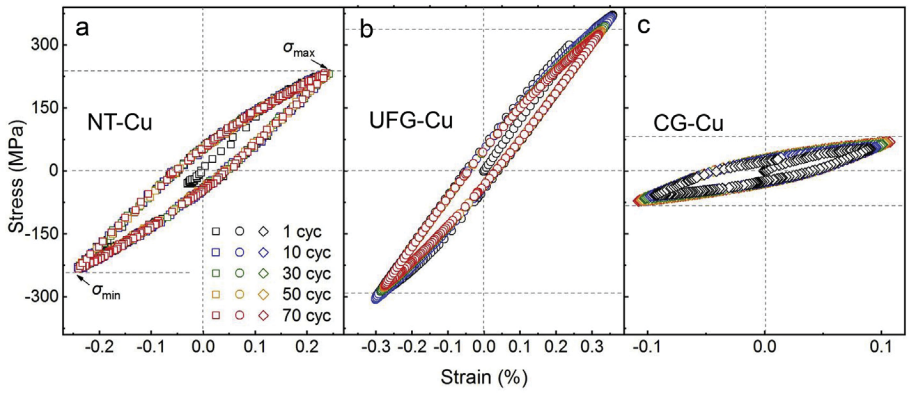

Fig. 1. Variation of stress-strain hysteresis of NT-Cu (a), UFG-Cu (b) and CG Cu (c) fatigued at the plastic strain amplitude ($\Delta\varepsilon_{pl}/2$) of 0.05% with number of cycles, showing symmetric response for NT-, UFG- and CG-Cu.

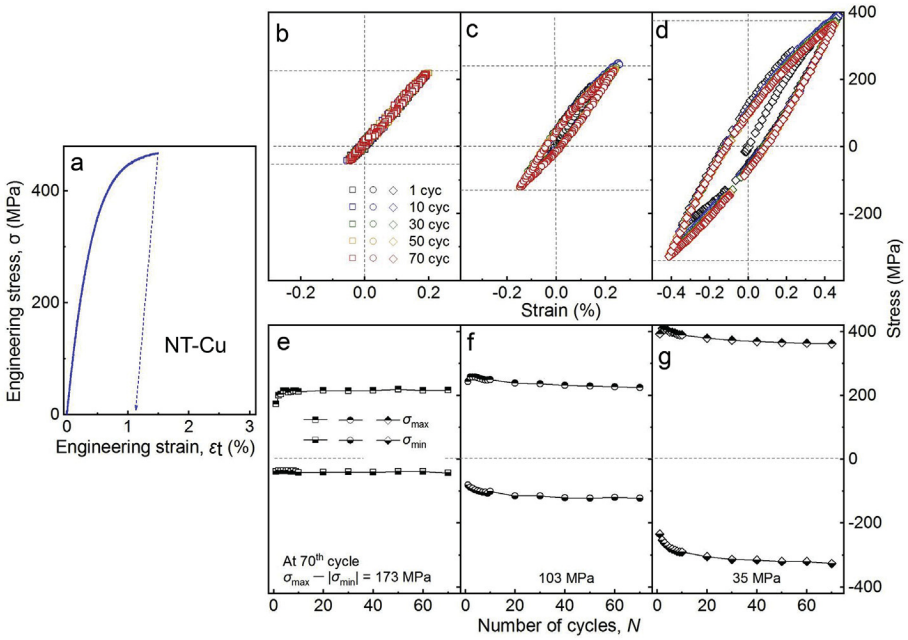

Fig. 2. Engineering stress-strain curve of tensile pre-deformation (a) and variation of stress-strain hysteresis loops (b, c, d) and cyclic stress (σ_{max}, σ_{min}) responses (e, f, g) with number of cycles for NT-Cu after a tensile predeformation strain of 1.5% when cyclically deformed at $\Delta\varepsilon_{pl}/2$ of 0.02%(b, e), 0.05%(c, f) and 0.15%(d, g), showing that the pre-deformation induces an asymmetric response in NT-Cu, which becomes more obvious at initial cycles and smaller $\Delta\varepsilon_{pl}/2$.

stress gap at 70th cycle from 103 to 35 MPa (Fig. 2f and g). As the stress gap is much smaller than σ_{max} and $|\sigma_{min}|$ at 70th cycle (361 and 326 MPa), symmetric cyclic response is considered to be reached for the tensile pre-deformed NT-Cu cyclically deformed at $\Delta\varepsilon_{pl}/2$ of 0.15%.

NT-Cu was also subjected to a larger tensile pre-strain of 3% (Fig. 3a) before three individual fully reversed tension-compression cyclic loading with $\Delta\varepsilon_{pl}/2$ of 0.02% (Fig. 3b and e), 0.05% (Fig. 3c and f) and 0.15% (Fig. 3d and g). Similar cyclic asymmetry with σ_{max} in tension larger than σ_{min} in compression was detected, especially at relatively smaller $\Delta\varepsilon_{pl}/2$. At larger $\Delta\varepsilon_{pl}/2$, the degree of cyclic asymmetry reduces with increasing number of cycles, and finally NT-Cu recovers to its symmetric cyclic response. For any given imposed $\Delta\varepsilon_{pl}/2$, the stress gap between σ_{max} and $|\sigma_{min}|$ for NT-Cu after a tensile pre-strain of 3% at 70th cycle is comparable to that of NT-Cu after a tensile pre-strain of 1.5%, suggesting that the

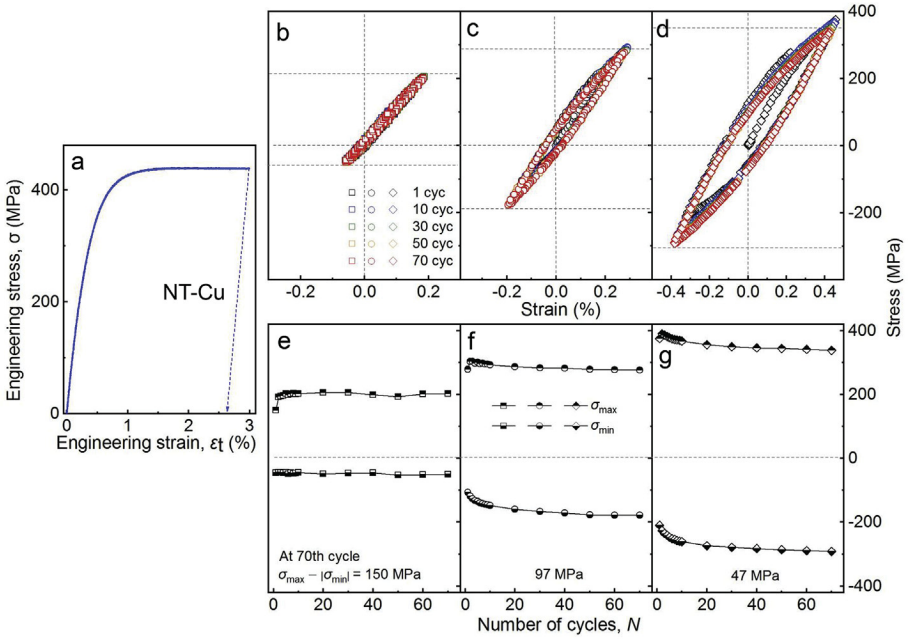

Fig. 3. Engineering stress-strain curve of tensile pre-deformation (a) and variation of stress-strain hysteresis loops (b, c, d) and cyclic stress (σ_{max}, σ_{min}) responses (e, f, g) with number of cycles for NT-Cu after a tensile predeformation strain of 3% when cyclically deformed at $\Delta\varepsilon_{pl}/2$ of 0.02% (b, e), 0.05% (c, f) and 0.15% (d, g), showing that the pre-deformation induces an asymmetric response in NT-Cu, which becomes more obvious at initial cycles and smaller $\Delta\varepsilon_{pl}/2$.

degree of cyclic asymmetry of NT-Cu may not be sensitive to the applied tensile pre-strain.

For comparison, a tensile pre-strain of 3% was also performed on UFG- (Fig. 4a) and CG-Cu (Fig. 4d), followed by tension-compression cyclic loading with $\Delta\varepsilon_{pl}/2$ of 0.05% (Fig. 4b-c and 4e-f). It is seen that the stress gap between σ_{max} and $|\sigma_{min}|$ for UFG-Cu after tensile pre-deformation decreases from 178 MPa at 1st cycle to 56 MPa at 70th cycle (Fig. 4b and c) which is comparable to that of UFG-Cu without tensile pre-deformation shown in Fig. 1b. For CG-Cu with pre-deformation, the stress gap between σ_{max} and $|\sigma_{min}|$ decreases from 62 MPa at 1st cycle to 13 MPa at 70th cycle (Fig. 4e and f). The easy recovery of cyclic symmetry observed in pre-deformed UFG- and CG-Cu is distinct from the obvious cyclic asymmetry of pre-deformed NT-Cu cyclically deformed at the same strain amplitude.

We have defined a stress ratio, $\sigma_{max}/|\sigma_{min}|$, to better quantify the cyclic asymmetry of NT-Cu after pre-deformation. The stress ratio is close to 1 for as-deposited NT-Cu at various $\Delta\varepsilon_{pl}/2$ (Fig. 5a), like that observed in fatigued CG and UFG counterparts (Fig. 5b) in this study and reported in the literature [8,26,30,48,53]. The stress ratio deviates from 1 for NT-Cu with pre-deformation: it becomes larger for smaller $\Delta\varepsilon_{pl}/2$, which is more obvious than that observed in CG and UFG counterparts under the same conditions (Fig. 5). When the imposed $\Delta\varepsilon_{pl}/2$ is sufficiently large (i.e. $\Delta\varepsilon_{pl}/2 = 0.15\%$), the stress ratio of tensile pre-deformed NT-Cu decreases with increasing number of cycles, indicating a gradual recovery to cyclic symmetry due to cyclic deformation.

3.3. Simulated cyclic response of tensile pre-deformed NT-Cu and twin-free Cu

In parallel to experimental investigations, MD simulations were performed to demonstrate the tensile pre-deformation effect on the cyclic response of NT-Cu. The tensile pre-deformation strain in MD simulations is selected to be 15% to ensure a sufficiently large initial dislocation density (on the order of $1 \times 10^{17}\,m^{-2}$) in the system before subsequent cyclic tests. After tensile pre-deformation (Fig. 6a), we measured the stress-strain hysteresis loops of NT-Cu at three different cyclic total strain amplitudes of $\Delta\varepsilon_t/2 = 0.5\%$, 1% and 2% (Fig. 6b–d). By measuring half of the width of the simulated hysteresis loops at zero stress, the corresponding plastic strain amplitudes of simulated NT-Cu can be approximated as $\Delta\varepsilon_{pl}/2 = 0.05\%$, 0.15% and 0.30%, which is almost comparable to those applied in our experimental work. We then extracted and plotted the maximum and the minimum stresses, σ_{max} and σ_{min}, during each cycle for each $\Delta\varepsilon_t/2$ (Fig. 6e–g). As in our experiments, we computed the stress ratio of $|\sigma_{max}/\sigma_{min}|$ and used it as a measure of the cyclic asymmetry of the pre-deformed sample. Fig. 7a shows the evolution of the stress ratio with respect to the number of cycles N. During the first few cycles, the stress ratio changes as the dislocation structure in the tensile pre-deformed NT-Cu sample is unstable. At $N = 10$, the cyclic response reaches saturation and exhibits clear asymmetry at $\Delta\varepsilon_t/2 = 0.5\%$ and 1%. Increasing $\Delta\varepsilon_t/2$ to 2% leads to a much-reduced asymmetry in the cyclic response of the tensile pre-deformed NT-Cu sample. The transition from cyclic asymmetry to cyclic symmetry as the cyclic strain amplitude increases is consistent with our experimental results (Fig. 5a). It is noted that the variation trends in Figs. 5a and 7a at the beginning of cyclic tests are different, which might be caused by the large discrepancy in grain size and strain rate between experiments and simulations.

For comparison, we applied 15% of tensile pre-deformation strain on twin-free Cu sample (Fig. 8a) and examined its subsequent cyclic response at three different cyclic total strain

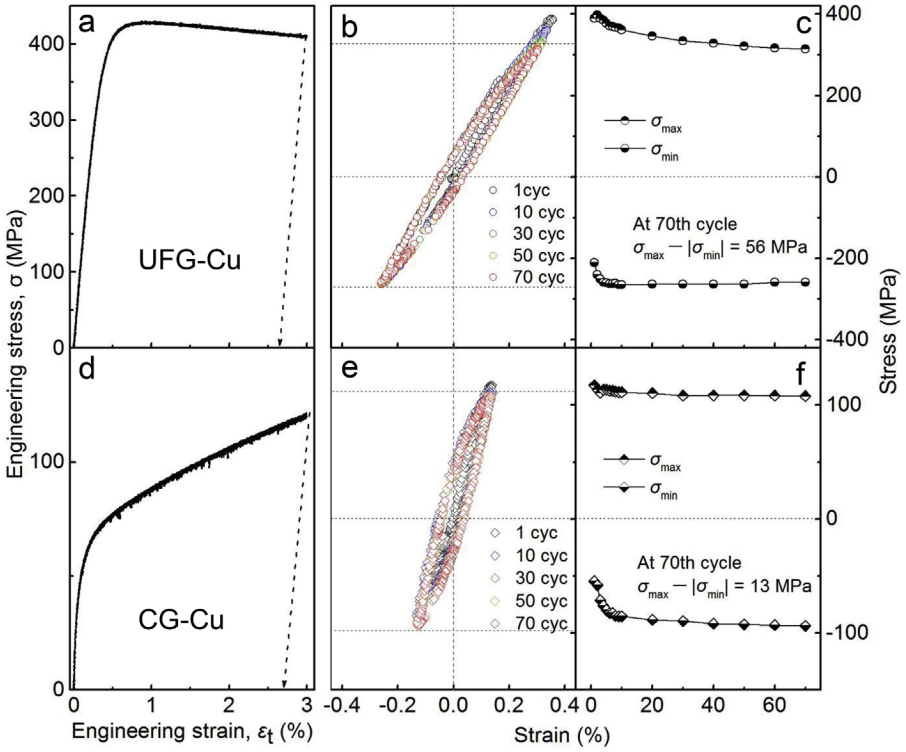

Fig. 4. Engineering stress-strain curve of tensile pre-deformation (a, d), variation of stress-strain hysteresis loops (b, e) and cyclic stress (σ_{max}, σ_{min}) responses (e, f) with number of cycles for UFG- (a, b, c) and CG-Cu (d, e, f) after a tensile pre-deformation strain of 3% when cyclically deformed at $\Delta\varepsilon_{pl}/2$ of 0.05%, showing the asymmetric response of UFG- and CG-Cu was promptly recovered to be symmetric within 70 cycles.

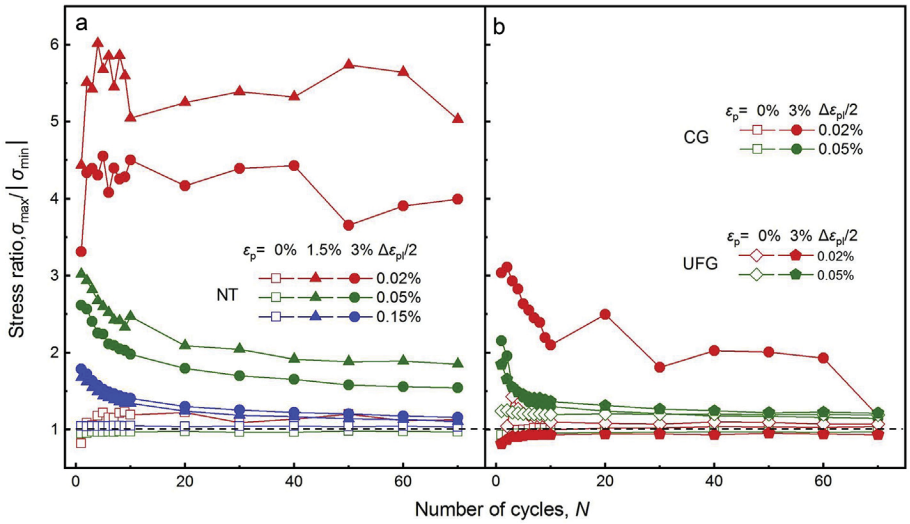

Fig. 5. Cyclic strain amplitude effects on stress ratio ($\sigma_{max}/|\sigma_{min}|$) responses of NT- (a), UFG- and CG-Cu (b) without and after tensile pre-deformation strains of 1.5% and 3%, showing that at the larger imposed strain amplitude, the smaller stress ratio can be detected in NT-Cu after tensile pre-deformation.

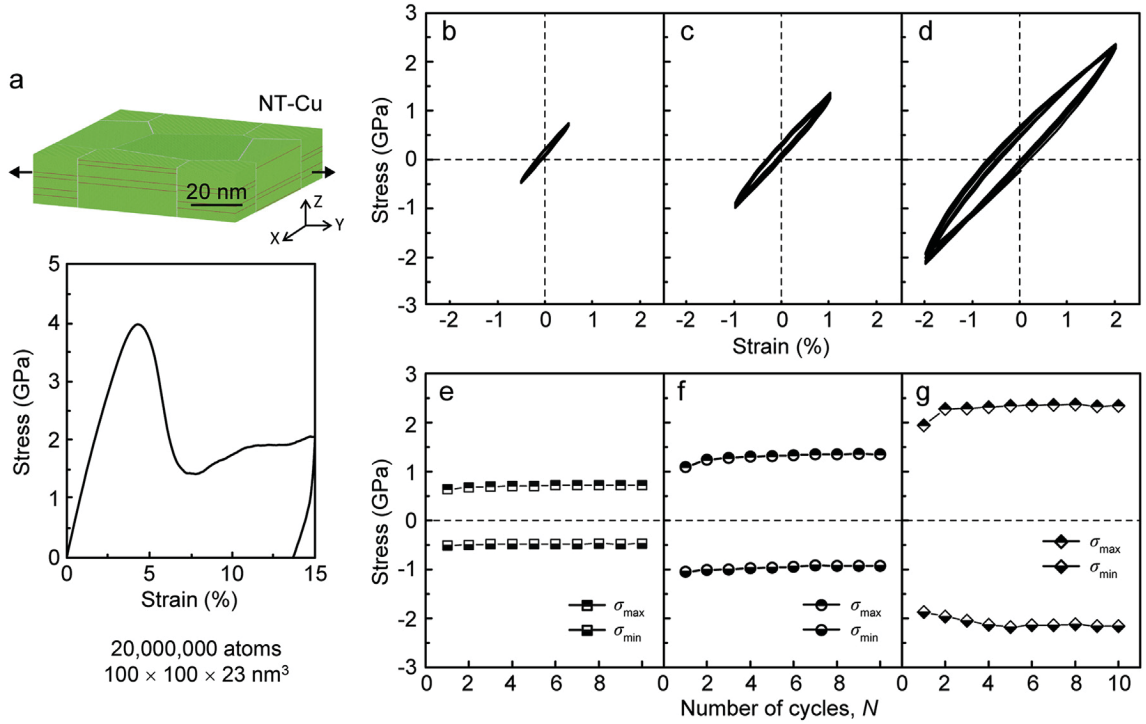

Fig. 6. (a) Tensile pre-deformation simulation setup and stress-strain curve of NT-Cu. (b–d) Stress-strain hysteresis loops of NT-Cu after tensile pre-deformation at cyclic total strain amplitudes ($\Delta\varepsilon_t/2$) of 0.5%, 1% and 2%. (e–g) Variation of cyclic stresses, σ_{max} and σ_{min}, with the number of cycles at corresponding $\Delta\varepsilon_t/2$.

amplitudes $\Delta\varepsilon_t/2 = 0.5\%$, 1% and 2% (Fig. 8b–g). The corresponding stress-strain hysteresis loops are shown in Fig. 8b–d, and the variation of σ_{max} and σ_{min} with respect to the number of cycles N is shown in Fig. 8e–g. The plastic strain amplitudes of simulated twin-free Cu at $\Delta\varepsilon_t/2$ are estimated as $\Delta\varepsilon_{pl}/2 = 0.15\%$, 0.25% and 0.80% from the simulated hysteresis loops, respectively. When the cyclic response saturates, we found much smaller stress ratios in tensile pre-deformed twin-free Cu sample than those observed in tensile pre-deformed NT-Cu for all three strain amplitudes (Fig. 7), indicating that the nanotwins and the associated deformation mechanisms must play an important role in the asymmetric cyclic response of the tensile pre-deformed NT-Cu sample.

4. Discussion

The hysteresis loops of as-deposited and tensile pre-deformed NT-Cu samples during cyclic loading exhibit, besides the usual well-known Bauschinger effect, with reduced elastic limits upon stress reversal from tension to compression and vice versa [1,54], a very strong stress asymmetry in tension and in compression. Compared to the symmetric cyclic stress response of the as-deposited NT-Cu and other materials [1], this markedly

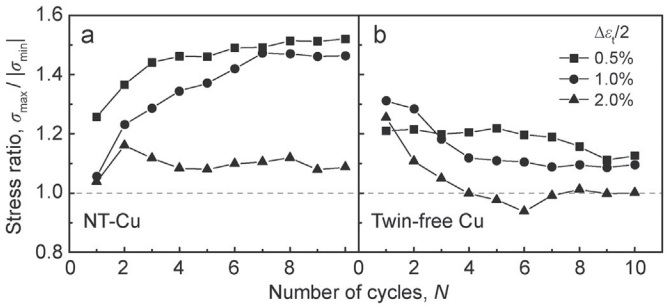

Fig. 7. Variation of stress ratio, $|\sigma_{max}/\sigma_{min}|$, with respect to the number of cycles for simulated NT (a) and twin-free (b) Cu at various cyclic total strain amplitudes after tensile pre-deformation.

asymmetric tension-compression response of the tensile pre-deformed NT-Cu is a characteristic feature of the pre-strained material. For this reason, the cyclic stress asymmetry and the underlying microstructural mechanisms were analyzed in some detail.

In order to uncover the mechanisms of tensile pre-deformation induced cyclic asymmetry of NT-Cu, we have examined the microstructures of NT-Cu after tensile pre-deformation and then fatigue tests at different strain amplitudes, using a two-beam diffraction technique in TEM [38]. After a tensile pre-deformation strain of 1.5%, we detected a high density of short dislocation segments overlapping with the moiré fringes of twin planes in NT-Cu (Fig. 9a) under a diffraction vector $\boldsymbol{g} = [-200]$ from the matrix (Fig. 9d). Previous studies have demonstrated that these dislocation segments are projections of misfit tails of threading dislocations in tensile-deformed NT-Cu [36,37]. It is clear that the threading dislocations are randomly distributed in the nanotwins after tensile pre-deformation, with different numbers of segments in different twins, as highlighted by the black rectangles 1 & 2 in Fig. 9a.

Imposing a small plastic strain amplitude ($\Delta\varepsilon_{pl}/2 = 0.02\%$) on the tensile pre-deformed NT-Cu does not obviously change the dislocation structures in nanotwins. Subsequent cyclic deformation at $\Delta\varepsilon_{pl}/2$ of 0.02% is still dominated by randomly distributed threading dislocations (Fig. 9b).

In contrast, imposing a sufficiently large plastic strain amplitude ($\Delta\varepsilon_{pl}/2 = 0.15\%$) leads to reorganization of the short dislocation segments in tensile pre-deformed NT-Cu. We observed a uniform pattern of dislocations with roughly equal interspacing after cyclic deformation (marked by the dashed lines in Fig. 9c). Previous studies have demonstrated that such uniform patterning of short dislocation segments in nanotwins represents a deformation mechanism via CNDs observed in as-deposited NT-Cu after cyclic deformation [24]. The formation of CNDs is caused by the linking of misfit tails of threading dislocations in adjacent nanotwins of the tensile pre-deformed NT-Cu under cyclic deformation. The movement of threading dislocations and CNDs in the nanotwins is not supposed to destroy the stability of NT structure [23,24]. We verified this by examining the morphology of nanotwins and twin/grain sizes of the tensile pre-deformed NT-Cu during cyclic deformation at either small or large $\Delta\varepsilon_{pl}/2$.

We have also adopted MD simulations to probe the underlying atomistic mechanism responsible for the effect of tensile pre-deformation on the cyclic response of NT-Cu observed in both experiments and MD simulations. During tensile pre-deformation, plastic deformation is governed by the activation and movement of threading dislocations in individual nanotwin layers (Fig. 10a). It is known that each threading dislocation is composed of a dislocation segment gliding between two neighboring twin planes and two misfit tail dislocations lying on the twin planes [43]. Once formed during tensile pre-deformation, the movement of a threading dislocation during subsequent cyclic deformation is asymmetric (Fig. 10b). During the tension stage of a loading cycle,

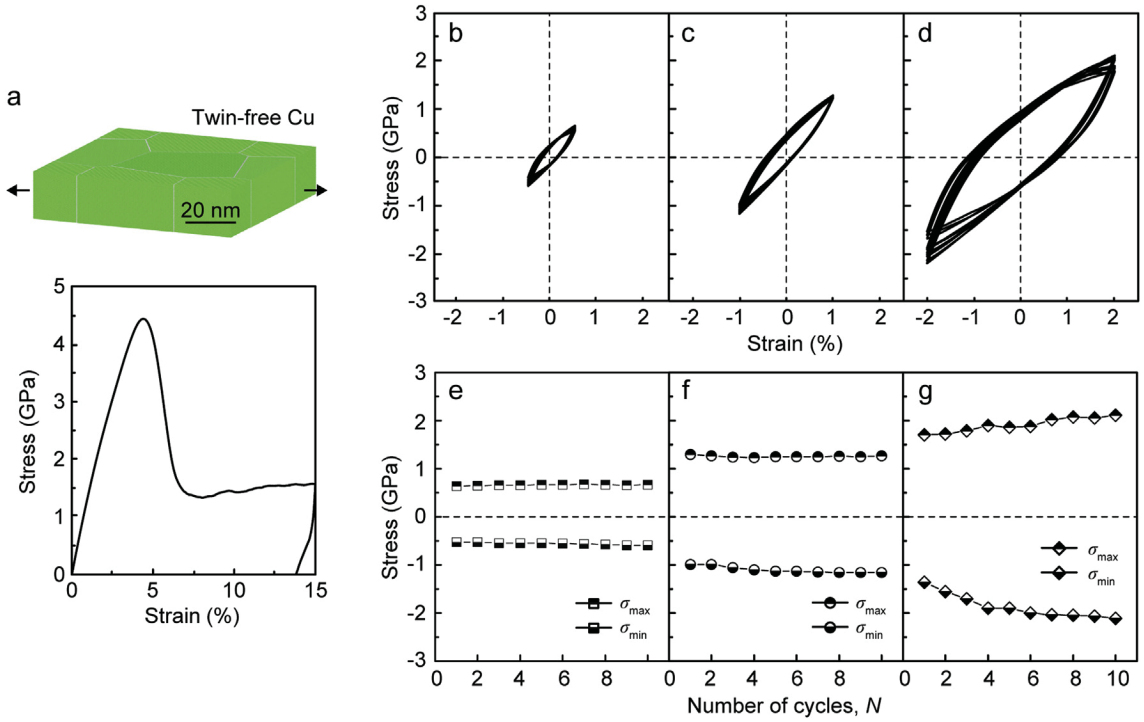

Fig. 8. (a) Tensile pre-deformation simulation setup and stress-strain curve of twin-free Cu. (b–d) Stress-strain hysteresis loops of twin-free Cu after tensile pre-deformation at $\Delta\varepsilon_t/2$ of 0.5%, 1% and 2%. (e–g) Variation of cyclic stresses, σ_{max} and σ_{min}, with the number of cycles at corresponding $\Delta\varepsilon_t/2$.

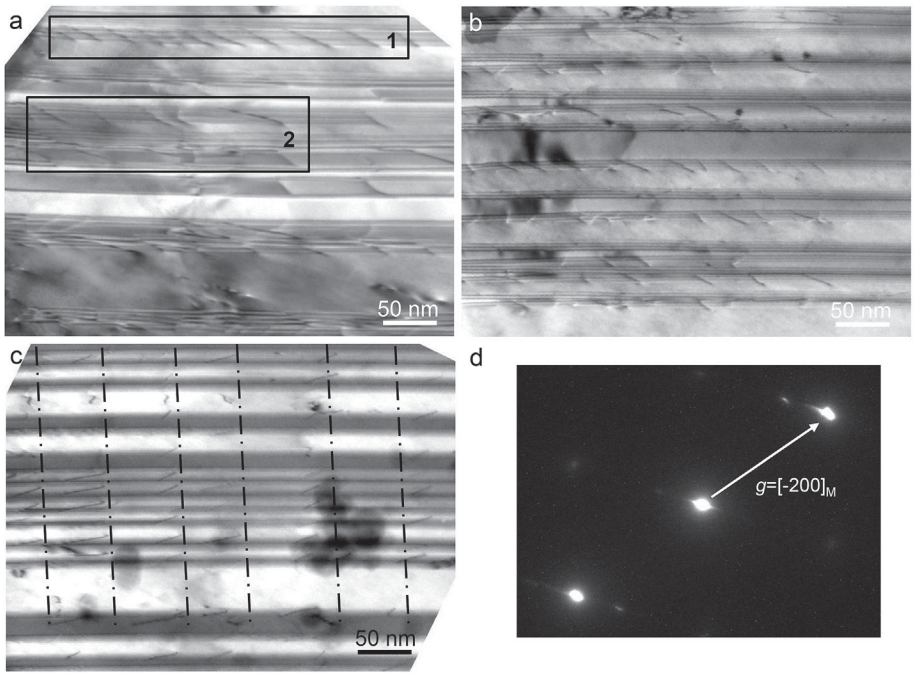

Fig. 9. Cross-sectional TEM images of NT-Cu after a tensile pre-deformation strain of 1.5% (a), then followed by cyclic deformation tests at $\Delta\varepsilon_{pl}/2$ of 0.02% (b) and (c) 0.15% with number of 70 cycles, under two beam diffraction mode (with $g=[-200]_M$ (d)), showing that randomly distributed threading dislocations during tensile predeformation tests gradually change to uniformly distributed correlated necklace dislocations.

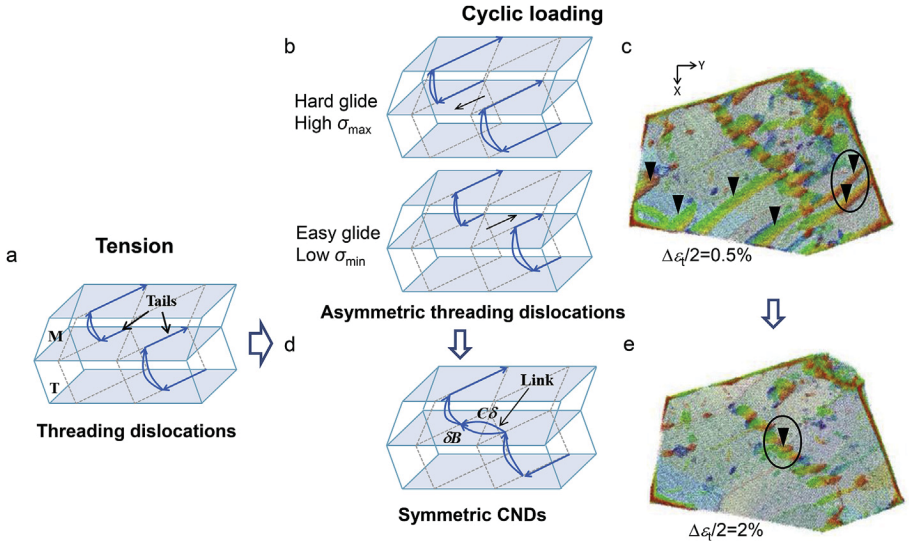

Fig. 10. MD simulation of cyclic deformation of NT Cu after tension pre-deformation. (a) Schematic of threading dislocations with asymmetric structure activated during tensile pre-deformation, causing asymmetric cyclic response (b). (c) Snapshot of long tails of threading dislocations in MD simulation of NT Cu cyclically deformed at $\Delta\varepsilon_t/2=0.5\%$, indicated by black arrows. (d) Schematic of CNDs with symmetric structure coming from the linkage of threading dislocations, leading to symmetric cyclic response. (e) Snapshot of CNDs in MD simulation of NT-Cu cyclically deformed at $\Delta\varepsilon_t/2=2\%$, indicated by the black arrow. The structures of dislocations highlighted by the black circle in (c, e) are illustrated in (a, d), respectively. Colors are assigned to atoms based on their out-of-plane spatial position in (c, e).

the threading dislocation tends to extend its misfit tails on the twin planes. We name it as "hard glide" as it is energetically more unfavorable and requires a positive stress σ_{max} with higher magnitude. On the other hand, when the external loading is reversed (e.g., the compression stage of a loading cycle), the threading dislocation moves backwards such that the length of the misfit tails decreases. This is called "easy glide" direction in the fatigue tests as it is energetically more favorable and it leads to a negative stress σ_{min} with lower magnitude (Movie 1). Thus, both our experiments and simulations indicate that the observed tension-compression asymmetric response behavior of tensile pre-deformed NT-Cu can be attributed to the directional nature of the resistance to the motion of threading dislocation, analogous to that reported in thin fcc metal film [54–56].

Supplementary video related to this article can be found at https://doi.org/10.1016/j.actamat.2019.06.026.

We must emphasize here that nanoscale twin spacing is of key importance to the occurrence of cyclic asymmetry in NT-Cu. If the

twin spacing is too thick to confine other slip systems, secondary or multiple slip systems could be activated aside from threading dislocations, forming dislocation patterns such as dislocation cell structures [57], like those observed in cyclically deformed CG metals [1,25,48]. Only at the nanometer scale could the twin lamella guarantee the activation of a single slip system of threading dislocations with long tails in tensile tests, leading to their hard and easy glide during subsequent tension-compression fatigue tests. From this point of view, the tension-compression asymmetry could not occur in metals with micron scale twins.

MD simulations revealed that at the cyclic strain amplitude of $\Delta\varepsilon_t/2 = 0.5\%$, there are numerous threading dislocations in the NT-Cu sample (indicated by black arrows in Fig. 10c). This may explain the asymmetric cyclic response of the tensile pre-deformed NT-Cu sample at $\Delta\varepsilon_t/2 = 0.5\%$ as both the structure and the glide of threading dislocations are cyclically asymmetric. The observed more obvious cyclic asymmetry with larger stress ratio in experiments than in MD simulations is most likely owing to threading dislocation with longer misfit tails in micron-scale twin channels than in simulated NT-Cu with much smaller grains.

At $\Delta\varepsilon_t/2 = 2\%$, we found that the cyclic deformation of NT-Cu is governed by CNDs and threading dislocation is rarely observed (Fig. 10e), consistent with that observed in Fig. 9c. It is expected that increasing the applied cyclic total strain amplitude from 0.5% to 2% promotes CND formation and leads to an exhaustion of threading dislocations in the tensile pre-deformed NT-Cu sample. In contrast to the asymmetric structure of threading dislocations, the structure of CND is symmetric because the misfit tails of threading dislocations have merged during the formation process of CNDs, leading to pairs of twinning partial dislocation segments on twin planes (Fig. 10d). During cyclic deformation, CNDs move back and forth along the twin planes without a net increase in the length of the twinning partial dislocation segments. The movement of CNDs is thus symmetric during cyclic tension-compression loading. This may explain the symmetric cyclic response of the tensile pre-deformed NT-Cu sample at $\Delta\varepsilon_t/2 = 2\%$ as both the structure and the glide of CNDs are cyclically symmetric.

Both experimental and MD observations indicate that the tension-compression asymmetric response of tensile pre-deformed NT-Cu is caused by threading dislocations produced in tensile pre-deformation, while the transition from cyclic asymmetry to cyclic symmetry is attributed to the gradual formation of CNDs by correlating threading dislocation in neighboring twins during cyclic loading.

Additional MD simulations were performed to investigate the effect of compressive pre-deformation on the cyclic response of NT-Cu. After a total of 15% compressive strain, the sample was unloaded and subjected to cyclic tension-compression loading (Fig. 11a).

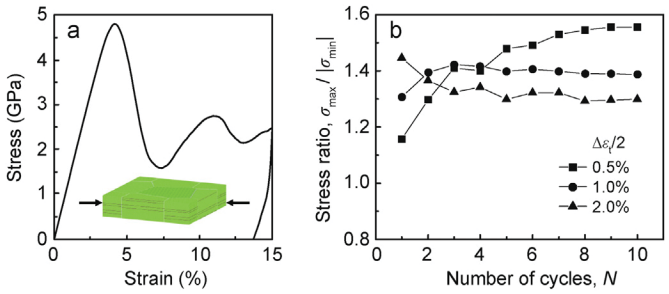

Fig. 11. MD simulation of NT Cu after compressive predeformation. (a) Engineering stress-strain curve of compressive predeformation, and (b) variation of stress ratio, $|\sigma_{min}/\sigma_{max}|$, with respect to the number of cycles at various cyclic total strain amplitudes for NT-Cu.

Cyclic asymmetry was observed for all three cyclic strain amplitudes $\Delta\varepsilon_t/2 = 0.5\%$, 1% and 2% (Fig. 11b). The stress ratio also decreases with increasing cyclic strain amplitudes, similar to that observed for tensile pre-deformed NT-Cu sample. At $\Delta\varepsilon_t/2 = 2\%$, the stress ratio measured for the compressive pre-deformed NT-Cu is somewhat larger than that measured for tensile pre-deformed NT-Cu (Fig. 8a). This could be attributed to the difference in sample and grain sizes along the loading direction in these two scenarios. Overall, our additional MD simulations have confirmed that the competition between threading dislocation-induced asymmetric cyclic response and CND-governed symmetric cyclic response is intrinsic to highly oriented NT-Cu samples subjected to pre-deformation.

Finally, we would like to emphasize that the cyclic asymmetry/symmetry can be viewed as an important concept, not only because it is closely correlated with the cyclic deformation mechanism of metals, but also because of its essential influence on material and component design, processing technique, performance and safety in application.

5. Conclusion

The effect of tensile pre-deformation on cyclic behavior of bulk polycrystalline Cu with highly oriented nanoscale twins has been investigated by both experiments and molecular dynamics simulations. NT-Cu after tensile pre-deformation exhibits tension-compression asymmetry with the magnitude of the maximum stress in tension much larger than that of the minimum stress in compression, which is distinct from cyclic symmetry typically observed in as-deposited NT-Cu and conventional f.c.c. CG and UFG metals. We revealed that the cyclic asymmetric response of tensile pre-deformed NT-Cu is owing to the asymmetric structure of threading dislocations with long misfit dislocation tails lying on the TBs. The reduction in cyclic asymmetry with increasing strain amplitudes and cyclic numbers is associated with the transition from threading dislocations to CNDs during cyclic deformation. These findings deepen our understanding of the fatigue behavior of NT metals and may provide insights/guidelines on tailor-designing fatigue-resistant engineering structures.

Acknowledgments

The authors acknowledge financial support by National Science Foundation of China (Grant Numbers. 51420105001, 51471172, 51601196 and U1608257) and the Key Research Program of Frontier Science, CAS. H.G. acknowledges support by NSF through Grant DMR-1709318. Q.P. acknowledges support by Youth Innovation Promotion Association CAS (Grant Number. 2019196). H.Z. acknowledges support by Zhejiang University through "Hundred Talents Program". The simulations reported were performed on resources provided by the Extreme Science and Engineering Discovery Environment (XSEDE) through Grant MS090046. The authors are grateful to Prof. Z.G. Wang, Dr. C. Kirchlechner for the insightful discussions and Mr. S. Jin for the sample preparation.

Appendix A. Supplementary data

Supplementary data related to this article can be found at https://doi.org/10.1016/j.actamat.2019.06.026.

References

[1] S. Suresh, Fatigue of Materials, second ed., Cambridge University Press, Cambridge, 1998.
[2] A.W. Thompson, W.A. Backofen, Effect of grain size on fatigue, Acta Metall. 19

(1971) 597–606.
[3] M.A. Meyers, A. Mishra, D.J. Benson, Mechanical properties of nanocrystalline materials, Prog. Mater. Sci. 51 (2006) 427–556.
[4] H. Mughrabi, H.W. Höppel, Cyclic deformation and fatigue properties of very fine-grained metals and alloys, Int. J. Fatigue 32 (2010) 1413–1427.
[5] T. Hanlon, Y.N. Kwon, S. Suresh, Grain size effects on the fatigue response of nanocrystalline metals, Scripta Mater. 49 (2003) 675–680.
[6] A. Vinogradov, S. Hashimoto, Multiscale phenomena in fatigue of ultra-fine grain materials - an overview, Mater. Trans., JIM 42 (2001) 74–84.
[7] P. Lukáš, L. Kunz, M. Svoboda, Fatigue mechanisms in ultrafine-grained copper, Kovove Mater 47 (2009) 1–9.
[8] H.W. Höppel, M. Brunnbauer, H. Mughrabi, Cyclic deformation behaviour of utrafine-grained size copper produced by equal channel angular pressing, in: Werkstoffwoche-Partnerschaft (Ed.), Proceedings of Materials Week 2000, Frankfurt, 2000, pp. 1–8.
[9] S.R. Agnew, A.Y. Vinogradov, S. Hashimoto, J.R. Weertman, Overview of fatigue performance of Cu processed by severe plastic deformation, J. Electron. Mater. 28 (1999) 1038–1044.
[10] A. Pineau, A. Amine Benzerga, T. Pardoen, Failure of metals III: fracture and fatigue of nanostructured metallic materials, Acta Mater. 107 (2016) 508–544.
[11] L. Lu, Y.F. Shen, X.H. Chen, L.H. Qian, K. Lu, Ultrahigh strength and high electrical conductivity in copper, Science 304 (2004) 422–426.
[12] K. Lu, L. Lu, S. Suresh, Strengthening materials by engineering coherent internal boundaries at the nanoscale, Science 324 (2009) 349–352.
[13] X. Zhang, H. Wang, X.H. Chen, L. Lu, K. Lu, R.G. Hoagland, A. Misra, High-strength sputter-deposited Cu foils with preferred orientation of nanoscale growth twins, Appl. Phys. Lett. 88 (2006) 173116.
[14] A.M. Hodge, Y.M. Wang, T.W. Barbee, Mechanical deformation of high-purity sputter-deposited nano-twinned copper, Scripta Mater. 59 (2008) 163–166.
[15] D.C. Jang, X.Y. Li, H.J. Gao, J.R. Greer, Deformation mechanisms in nanotwinned metal nanopillars, Nat.Nanotechnol. 7 (2012) 594–601.
[16] Y.M. Wang, F. Sansoz, T. LaGrange, R.T. Ott, J. Marian, T.W. Barbee Jr., A.V. Hamza, Defective twin boundaries in nanotwinned metals, Nat. Mater. 12 (2013) 697–702.
[17] D.C. Bufford, Y.M. Wang, Y. Liu, L. Lu, Synthesis and microstructure of electrodeposited and sputtered nanotwinned face-centered-cubic metals, MRS Bull. 41 (2016) 286–291.
[18] T. Zhu, H.J. Gao, Plastic deformation mechanism in nanotwinned metals: an insight from molecular dynamics and mechanistic modeling, Scripta Mater. 66 (2012) 843–848.
[19] K. Lu, Stabilizing nanostructures in metals using grain and twin boundary architectures, Nat. Rev. Mater. 1 (2016) 16019.
[20] C.J. Shute, B.D. Myers, S. Xie, S.Y. Li, T.W. Barbee Jr., A.M. Hodge, J.R. Weertman, Detwinning, damage and crack initiation during cyclic loading of Cu samples containing aligned nanotwins, Acta Mater. 59 (2011) 4569–4577.
[21] Q.S. Pan, Q.H. Lu, L. Lu, Fatigue behavior of columnar-grained Cu with preferentially oriented nanoscale twins, Acta Mater. 61 (2013) 1383–1393.
[22] A. Singh, L. Tang, M. Dao, L. Lu, S. Suresh, Fracture toughness and fatigue crack growth characteristics of nanotwinned copper, Acta Mater. 59 (2011) 2437–2446.
[23] Q.S. Pan, L. Lu, Strain-controlled cyclic stability and properties of Cu with highly oriented nanoscale twins, Acta Mater. 81 (2014) 248–257.
[24] Q.S. Pan, H.F. Zhou, Q.H. Lu, H.J. Gao, L. Lu, History-independent cyclic response of nanotwinned metals, Nature 551 (2017) 214–217.
[25] P. Peralta, C. Laird, Fatigue of metals, in: D.E. Laughlin, K. Hono (Eds.), Physical Metallurgy, fifth ed., Elsevier, Oxford, Oxford, 2014, pp. 1765–1880.
[26] H. Mughrabi, Cyclic hardening and saturation behavior of copper single-crystals, Mater. Sci. Eng. 33 (1978) 207–223.
[27] X.W. Li, Z.G. Wang, G.Y. Li, S.D. Wu, S.X. Li, Cyclic stress-strain response and surface deformation features of [011] multiple-slip-oriented copper single crystals, Acta Mater. 46 (1998) 4497–4505.
[28] R. Wang, H. Mughrabi, Secondary cyclic hardening in fatigued copper monocrystals and polycrystals, Mater. Sci. Eng. 63 (1984) 147–163.
[29] J. Polák, K. Obrtlik, J. Helesic, Cyclic strain localization in polycrystalline copper at room-temperature and low-temperatures, Mater. Sci. Eng. A 132 (1991) 67–76.
[30] C.E. Feltner, C. Laird, Cyclic stress-strain response of FCC metals and alloys 1. phenomenological experiments, Acta Metall. 15 (1967) 1621–1632.
[31] C. Laird, J.M. Finney, A. Schwartzman, R.D.L. Veaux, History dependence in cyclic stress-strain response of wavy slip materials, J. Test. Eval. 3 (1975) 435–441.
[32] H.J. Christ, G. Hoffmann, O. Ottinger, History effects in metals during constant and variable amplitude testing .1. Wavy dislocation glide behavior, Mater. Sci. Eng. A 201 (1995) 1–12.
[33] P. Lukáš, M. Klesnil, Cyclic stress-strain response and fatigued life of metals in low amplitude region, Mater. Sci. Eng. 11 (1973) 345–356.
[34] J. Schijve, Fatigue of Structures and Materials, second ed., Springer, Netherlands, 2009.
[35] C.E. Feltner, C. Laird, Cyclic stress-strain response of F.C.C. metals and alloys–II Dislocation structures and mechanisms, Acta Metall. 15 (1967) 1633–1653.
[36] Z.S. You, L. Lu, K. Lu, Tensile behavior of columnar grained Cu with preferentially oriented nanoscale twins, Acta Mater. 59 (2011) 6927–6937.
[37] Q.H. Lu, Z.S. You, X.X. Huang, N. Hansen, L. Lu, Dependence of dislocation structure on orientation and slip systems in highly oriented nanotwinned Cu, Acta Mater. 127 (2017) 85–97.
[38] D.B. Williams, C.B. Carter, Transmission Electron Microscopy: A Textbook for Materials Science, second ed., Springer Science/Business Media, New York, 2009.
[39] S. Nose, A unified formation of the constant temperature molecular-dynamic methods, J. Chem. Phys. 81 (1984) 511–519.
[40] W.G. Hoover, Constant-pressure equations of motion, Phys. Rev. 34 (1986) 2499–2500.
[41] Y. Mishin, M.J. Mehl, D.A. Papaconstantopoulos, A.F. Voter, J.D. Kress, Structural stability and lattice defects in copper: Ab initio, tight-binding, and embedded-atom calculations, Phys. Rev. B 63 (2001) 224106.
[42] D. Faken, H. Jonsson, Systematic analysis of local atomic structure combined with 3D computer graphics, Comput. Mater. Sci. 2 (1994) 279–286.
[43] H.F. Zhou, X.Y. Li, S.X. Qu, W. Yang, H.J. Gao, A jogged dislocation governed strengthening mechanism in nanotwinned metals, Nano Lett. 14 (2014) 5075–5080.
[44] H.F. Zhou, H.J. Gao, A plastic deformation mechanism by necklace dislocations near crack-like defects in nanotwinned metals, J. Appl. Mech.-Trans. ASME 82 (2015) 5.
[45] X.Y. Li, Y.J. Wei, L. Lu, K. Lu, H.J. Gao, Dislocation nucleation governed softening and maximum strength in nano-twinned metals, Nature 464 (2010) 877–880.
[46] J. Schiøtz, K.W. Jacobsen, A maximum in the strength of nanocrystalline copper, Science 301 (2003) 1357–1359.
[47] Z.S. Basinski, S.J. Basinski, Fundamental aspects of low amplitude cyclic deformation in face-centred cubic crystals, Prog. Mater. Sci. 36 (1992) 89–148.
[48] A.T. Winter, Model for fatigue of copper at low plastic strain amplitudes, Philos. Mag. A 30 (1974) 719–738.
[49] J.D. Morrow, Cyclic plastic strain Energy and fatigue of metals, in: B.J. Lazan (Ed.), Internal Friction, Damping, and Cyclic Plasticity ASTM STP 378, American Society for Testing of Materials, Philadelphia, 1965, pp. 45–87.
[50] N.Y. Jin, Formation of dislocation structures during cyclic deformation of F.C.C. crystals–I. Formation of PSBs in crystals oriented for single-slip, Acta Metall. 37 (1989) 2055–2066.
[51] C.D. Liu, D.X. You, M.N. Bassim, Cyclic strain hardening in polycrystalline copper, Acta Metall. Mater. 42 (1994) 1631–1638.
[52] D.J. Morrison, V. Chopra, Cyclic stress-strain response of polycrystalline nickel, Mater. Sci. Eng. A 177 (1994) 29–42.
[53] K.V. Rasmussen, O.B. Pedersen, Fatigue of copper polycrystals at low plastic strain amplitudes, Acta Metall. 28 (1980) 1467–1478.
[54] Y. Xiang, J.J. Vlassak, Bauschinger and size effects in thin-film plasticity, Acta Mater. 54 (2006) 5449–5460.
[55] S.P. Baker, R.M. Keller-Flaig, J.B. Shu, Bauschinger effect and anomalous thermomechanical deformation induced by oxygen in passivated thin Cu films on substrates, Acta Mater. 51 (2003) 3019–3036.
[56] P. Pant, K.W. Schwarz, S.P. Baker, Dislocation interactions in thin FCC metal films, Acta Mater. 51 (2003) 3243–3258.
[57] X.L. Guo, L. Lu, S.X. Li, Effects of twin size on the dislocation configuration during cyclic deformation of polycrystalline twin copper, Acta Metall. Sin. 41 (2005) 23–27.